

2010

Quantum Approach to Electronic Noise Calculations in the Presence of Electron-Phonon Interactions

Hong-Hyun Park
Purdue University

Gerhard Klimeck
gekco@purdue.edu

Follow this and additional works at: <http://docs.lib.purdue.edu/nanopub>

 Part of the [Nanoscience and Nanotechnology Commons](#)

Park, Hong-Hyun and Klimeck, Gerhard, "Quantum Approach to Electronic Noise Calculations in the Presence of Electron-Phonon Interactions" (2010). *Birck and NCN Publications*. Paper 515.
<http://docs.lib.purdue.edu/nanopub/515>

This document has been made available through Purdue e-Pubs, a service of the Purdue University Libraries. Please contact epubs@purdue.edu for additional information.

Quantum approach to electronic noise calculations in the presence of electron-phonon interactions

Hong-Hyun Park and Gerhard Klimeck

Electrical Engineering and Computer Science, Purdue University, West Lafayette, Indiana 47097, USA

(Received 10 May 2010; revised manuscript received 5 September 2010; published 29 September 2010)

A quantum-mechanical approach to the calculation of electronic noise for nanoscale devices is presented. This method is based on the nonequilibrium Green's-function formalism with electron-phonon scattering mechanisms and takes the effects of the Pauli exclusion principle and the long-range Coulomb interactions into account. As examples the drain current noise characteristics of silicon nanowire transistors at room temperature are simulated. The drain current noise in the saturation regime is primarily shot-noise dominant but is suppressed for higher gate biases due to the electron-electron correlation in the channel region. The role of electron-phonon interactions on noise, the transition from thermal to shot noise, and the physical origin of the shot-noise phenomenon are also investigated.

DOI: [10.1103/PhysRevB.82.125328](https://doi.org/10.1103/PhysRevB.82.125328)

PACS number(s): 73.63.Nm, 42.50.Lc

I. INTRODUCTION

Noise is one of the most important limiting factors in the operation of electronic systems. Since the signal-to-noise ratio of a system is determined by its device components, noise phenomena in electronic devices have been important issues in both theoretical and practical aspects. For conventional micron-scale semiconductor devices, various noise phenomena have been well understood and analyzed within the semiclassical transport point of view.¹⁻⁴ As electronic devices continue to scale down, quantum effects become significant in the noise as well as in the signal characteristics. Although the noise phenomena in nanoscale devices have been studied actively for about two decades,⁵⁻¹⁴ there are still many open issues that need to be addressed in the quantum transport point of view.

So far most quantum noise studies have been based on the scattering matrix approach, where the device is treated as a scattering target which transmit or reflect electrons.^{7,10} The scattering matrix approach clearly illuminates the random processes of electrons due to the injection from contacts, the tunneling through the device, and the effect of Pauli exclusion principle on noise. However, it fails to capture the effects of long-range Coulomb interactions on noise and cannot be applied in the presence of electron-phonon interactions inside the device. Recently a statistical version of the scattering matrix approach that considers the long-range Coulomb interactions was suggested, however, it is also valid only in the ballistic transport regime ignoring effects due to electron-phonon interactions.¹⁵ On the other hand, our previous study suggested another approach that is applicable even in the presence of electron-phonon interactions, however, it had neglected the effect of the long-range Coulomb interactions on noise.¹⁶

This paper presents a general approach to calculate the terminal current noise of nanoscale devices, which incorporates the scattering matrix approach and its statistical version as special cases. The method is based on the nonequilibrium Green's-function (NEGF) formalism with electron-phonon interactions and takes the effects of the Pauli exclusion principle and the long-range Coulomb interactions into account. Using this method we investigate the drain current noise

characteristics of silicon nanowire transistors (SNWTs) which have been studied as one of the possible candidate for future transistors. Our results show that the drain current noise is more like shot noise compared with that of conventional metal-oxide-semiconductor field-effect transistors (MOSFETs) and the drain current noise is significantly suppressed due to the electron-electron correlations in the channel region as the gate voltage becomes larger. We also explore the physical origin of shot-noise phenomenon of SNWTs and the role of electron-phonon interactions on noise.

This paper is organized as follows: in Sec. II the quantum theory of electronic noise based on the nonequilibrium formalism is presented. Section III gives the simulation results and discussions on the electronic noise in silicon nanowire transistors followed by conclusions in Sec. IV.

II. THEORY**A. Nonequilibrium Green's-function formalism**

This section briefly reviews the steady-state NEGF formalism with the effective-mass and Hartree approximations.¹⁷⁻¹⁹ For the sake of brevity a simplified notation without spin and valley states is used while our numerical implementation contains multiple valleys for silicon.

The governing equations for the retarded Green's function can be written as²⁰

$$[E - H^e(\mathbf{r}) - \Sigma^r(\mathbf{r}, E)]G^r(\mathbf{r}, \mathbf{r}'; E) = \delta(\mathbf{r} - \mathbf{r}'), \quad (1)$$

where $H^e(\mathbf{r})$ is the electron Hamiltonian

$$H^e(\mathbf{r}) = -\frac{\hbar^2}{2} \vec{\nabla} \cdot \left[\frac{1}{m^*(\mathbf{r})} \vec{\nabla} \right] + U(\mathbf{r}) \quad (2)$$

and $\Sigma^r(\mathbf{r}, E)$ is the retarded self-energy function

$$\Sigma^r(\mathbf{r}, E) = \frac{1}{2\pi} \int d\Gamma \frac{\Gamma(\mathbf{r}, E')}{E - E'}. \quad (3)$$

Here $m^*(\mathbf{r})$ is the effective mass, $U(\mathbf{r})$ is the self-consistent potential, and $\Gamma(\mathbf{r}, E) = \Gamma^{in}(\mathbf{r}, E) + \Gamma^{out}(\mathbf{r}, E)$ is the broadening

function given by the sum of individual contributions of phase-breaking processes such as electron-contact couplings and electron-phonon interactions. In this work the electron-phonon interactions are assumed to be spatially local and caused by a continuous distribution in space, resulting in the broadening functions as^{19,20}

$$\Gamma^{in}(\mathbf{r}, E) = \sum_{\alpha} \Gamma(\mathbf{r}_{\alpha}, E) f(\mathbf{r}_{\alpha}, E) + \int d\mathcal{E} D(\mathcal{E}) n(\mathbf{r}, E + \mathcal{E}), \quad (4)$$

$$\Gamma^{out}(\mathbf{r}, E) = \sum_{\alpha} \Gamma(\mathbf{r}_{\alpha}, E) [1 - f(\mathbf{r}_{\alpha}, E)] + \int d\mathcal{E} D(\mathcal{E}) p(\mathbf{r}, E - \mathcal{E}), \quad (5)$$

where the first term represents the electron-contact couplings and the second term represents the electron-phonon interactions. $\Gamma(\mathbf{r}_{\alpha}, E)$ is the broadening function for the contact α assuming a semi-infinite contact lead, and $f(\mathbf{r}_{\alpha}, E) = [e^{(E - \mu_{\alpha})/k_B T} + 1]^{-1}$ is the Fermi-Dirac distribution in contact α . The phonon interaction function $D(\mathcal{E})$ is given by^{19,20}

$$D(\mathcal{E}) = M(|\mathcal{E}|) \times \begin{cases} N(|\mathcal{E}|) & \text{if } \mathcal{E} < 0 \\ N(\mathcal{E}) + 1 & \text{if } \mathcal{E} > 0, \end{cases} \quad (6)$$

where the function $M(\mathcal{E})$ represents the electron-phonon interaction strength which involves the electron-phonon scattering mechanisms of the system and $N(\mathcal{E}) = [e^{\mathcal{E}/k_B T} - 1]^{-1}$ is the thermal equilibrium phonon number with energy \mathcal{E} . $n(\mathbf{r}, E)$ and $p(\mathbf{r}, E)$ are the electron and hole densities, respectively,²⁰

$$n(\mathbf{r}, E) = \frac{1}{2\pi} \int d\mathbf{r}' |G^r(\mathbf{r}, \mathbf{r}'; E)|^2 \Gamma^{in}(\mathbf{r}', E), \quad (7)$$

$$p(\mathbf{r}, E) = \frac{1}{2\pi} \int d\mathbf{r}' |G^r(\mathbf{r}, \mathbf{r}'; E)|^2 \Gamma^{out}(\mathbf{r}', E). \quad (8)$$

The above set of NEGF equations should be solved with the Poisson equation for self-consistency, and then the physical quantities implicated in the steady-state NEGF formalism can be obtained from the solution.

For the later discussions let us detail the motion of electrons involving phonon interactions. Since the electron-phonon interactions are assumed to be spatially local, electron fluxes can be decomposed into two kinds of elementary processes, coherent propagation and state transition. The coherent propagation of electrons from \mathbf{r}' to \mathbf{r} with energy E can be written as¹⁶

$$\begin{aligned} F^T(\mathbf{r}, \mathbf{r}'; E) &= \frac{1}{2\pi\hbar} |G^r(\mathbf{r}, \mathbf{r}'; E)|^2 \Gamma^{out}(\mathbf{r}, E) \Gamma^{in}(\mathbf{r}', E) \\ &= \frac{1}{2\pi\hbar} T(\mathbf{r}, \mathbf{r}'; E) [1 - f(\mathbf{r}, E)] f(\mathbf{r}', E), \end{aligned} \quad (9)$$

where $T(\mathbf{r}, \mathbf{r}'; E) = |G^r(\mathbf{r}, \mathbf{r}'; E)|^2 \Gamma(\mathbf{r}, E) \Gamma(\mathbf{r}', E)$ is transmission probability density and $f(\mathbf{r}, E) \equiv \Gamma^{in}(\mathbf{r}, E) / \Gamma(\mathbf{r}, E)$. The

state transition of electrons from E' to E at position \mathbf{r} can be written as¹⁶

$$F^T(\mathbf{r}; E, E') = \frac{1}{\hbar} D(E' - E) p(\mathbf{r}, E) n(\mathbf{r}, E'). \quad (10)$$

The terminal current is then obtained by the difference between the in-flux and out-flux of electrons through the contact as¹⁶

$$I_{\alpha} = \int dE \int \int_{\mathbf{r} \in \Omega_{\alpha}} d\mathbf{r} d\mathbf{r}' e [F^P(\mathbf{r}, \mathbf{r}'; E) - F^P(\mathbf{r}', \mathbf{r}; E)]. \quad (11)$$

In the ballistic limit the integrations of Eq. (11) are carried out in the contacts only and Eq. (11) reduces to the Landauer-Büttiker formula.

B. Noise calculation

This section describes the calculation of the current noise power of the contact α at the zero-frequency limit. In the noise calculations it is important to take the effects of the Pauli exclusion principle and the long-range Coulomb interactions into account. These kinds of electron-electron correlations are known to suppress the randomness of the propagation of electrons by introducing correlation among electrons.^{21,22} So far, most quantum noise theories included the Pauli exclusion principle but many of them failed to include the long-range Coulomb effect. The reason of that deficiency is that they use averaged values for carrier density while the effect of long-range Coulomb interactions on noise are the consequence of the random distribution of electrons in space which varies with time.

Recently a statistical approach to quantum noise calculations has been proposed in which many ensembles of different electron distributions are used to model the effect of long-range Coulomb interactions on noise.¹⁵ Although the work was performed only for the ballistic transport limit, its methodology to analyze noise statistically appears to be valid in general. We therefore take a similar statistical approach in this work.

For the statistical noise analysis we generate many ensembles by letting the occupation of contact states be completely empty or filled, each of which corresponds to one of the possible situations that might happen due to the particle nature of electrons. In doing so, the ensembles are generated randomly but the average of the occupation should be the same to that of a given steady state. Since the NEGF and Poisson equations are to be solved self-consistently for each ensemble, the distribution of the solution set reflects the effect of long-range Coulomb interactions on current.

The device current noise can be decomposed into contact and internal noise contributions. The contact noise is generated by the random injection of electrons from the contacts, and the internal noise is induced by the random occurrence of physical processes inside the device. Since the physical origins of these noise sources are uncorrelated, we can calculate them independently.

With regard to the contact noise contribution, the noise sources on the contacts are introduced explicitly in en-

sembles, so the fluctuation of terminal current in ensembles is directly related to the terminal current noise. From the statistical scattering matrix approach, the contact noise contribution can be written as the variance of the terminal current,¹⁵

$$S_{\alpha}^I = \frac{e^2}{\pi\hbar\Delta E} \text{var} \left\{ \int dE \int \int_{\mathbf{r} \in \Omega_{\alpha}} d\mathbf{r} d\mathbf{r}' T(\mathbf{r}, \mathbf{r}'; E) [f(\mathbf{r}', E) - f(\mathbf{r}, E)] \right\}, \quad (12)$$

where ΔE is the energy step used in the numerical calculations. According to Ref. 15 the choice of ΔE is related to the rate of convergence but the convergence itself is ensured in every case.

For the calculation of the internal noise contribution we need to figure out the random physical processes inside the device. In the ballistic transport limit the probabilistic transmission of electrons between the contacts is the only internal noise source, however, it is not so simple in the presence of electron-phonon interactions in which the scattering matrix approach fails. As mentioned in the previous section, the motion of electrons interacting with phonons can be depicted in terms of coherent propagations and state transitions. In the noise point of view each elementary flux will fluctuate around its dc value and affect to the terminal current noise. Hence the internal noise contribution will be obtained in two steps: the fluctuation power of each and every elementary flux is calculated first and then converted into the terminal current noise. Since electron-phonon interactions are assumed to occur independently, the simple summation of each fluctuation will give the internal noise contribution. For the conversion we introduce a transfer function $H_{\alpha}(\mathbf{r}, E)$ defined as a small-signal response in the electron flux out through the contact α to a unit electron in-scattering rate at (\mathbf{r}, E) .¹⁶ Due to the linearity of the small-signal analysis, the transfer function for the electron out-scattering at (\mathbf{r}, E) has the same magnitude as $H_{\alpha}(\mathbf{r}, E)$ but the opposite sign. With that a small amount of elementary flux between two phase-breaking sites can be characterized as simultaneous in-scattering and out-scattering of electrons at the two sites each, the fluctuation power of elementary flux between (\mathbf{r}, E) and (\mathbf{r}', E') can be converted into the terminal current noise with a factor of $[H_{\alpha}(\mathbf{r}, E) - H_{\alpha}(\mathbf{r}', E')]^2$. The way of calculating the transfer function from the steady-state NEGF formalism will be explained in the next section.

Fluctuations of coherent propagations stem from probabilistic transmissions of electrons, and its fluctuation power between positions \mathbf{r} and \mathbf{r}' with energy E can be modeled as

$$S^P(\mathbf{r}, \mathbf{r}'; E) = \frac{e^2}{\pi\hbar} T(\mathbf{r}, \mathbf{r}'; E) [1 - T(\mathbf{r}, \mathbf{r}'; E)] [f(\mathbf{r}, E) - f(\mathbf{r}', E)]^2, \quad (13)$$

which is from the partition noise contribution of the scattering matrix theory.¹⁰ The terminal current noise due to the fluctuation of coherent propagation is the sum of each contributions as

$$S_{\alpha}^P = \int dE \int \int_{|\mathbf{r}| \geq |\mathbf{r}'|} d\mathbf{r} d\mathbf{r}' \langle [H_{\alpha}(\mathbf{r}, E) - H_{\alpha}(\mathbf{r}', E)]^2 S^P(\mathbf{r}, \mathbf{r}'; E) \rangle, \quad (14)$$

where $\langle \dots \rangle$ represents the ensemble average and the restriction on the domain are inserted to avoid the duplication of noise sources.

Fluctuations of state transitions are caused by random interactions between electrons and phonons. If the interactions occur independently from one another as usually assumed, the fluctuation power of the state transition between energies E and E' at position \mathbf{r} can be written as²⁻⁴

$$S^T(\mathbf{r}; E, E') = 2e^2 [F^T(\mathbf{r}; E, E') + F^T(\mathbf{r}; E', E)]. \quad (15)$$

The terminal current noise due to the fluctuation of state transition is then obtained as

$$S_{\alpha}^T = \int d\mathbf{r} \int \int_{E \geq E'} dE dE' \langle [H_{\alpha}(\mathbf{r}, E) - H_{\alpha}(\mathbf{r}, E')]^2 S^T(\mathbf{r}; E, E') \rangle. \quad (16)$$

Finally the zero-frequency current noise power for the contact α is obtained as $S_{\alpha} = S_{\alpha}^I + S_{\alpha}^P + S_{\alpha}^T$. In the ballistic transport limit, S_{α}^T vanishes and the integrations of S_{α}^I and S_{α}^P are carried out over the contacts only, so the current noise power reduces to the statistical scattering matrix approach.

Note that calculating the transfer function for each ensemble is a huge computational burden. We therefore approximate the transfer function as static in ensembles for the sake of time, which is an adequate compromise unless the fluctuations induced by the contact injection is large. The current noise power can be written as

$$S_{\alpha} = \frac{e^2}{\pi\hbar\Delta E} \text{var} \left\{ \int dE \int \int_{\mathbf{r} \in \Omega_{\alpha}} d\mathbf{r} d\mathbf{r}' T(\mathbf{r}, \mathbf{r}'; E) [f(\mathbf{r}', E) - f(\mathbf{r}, E)] \right\} + \int dE \int \int_{|\mathbf{r}| \geq |\mathbf{r}'|} d\mathbf{r} d\mathbf{r}' [H_{\alpha}(\mathbf{r}, E) - H_{\alpha}(\mathbf{r}', E)]^2 \langle S^P(\mathbf{r}, \mathbf{r}'; E) \rangle + \int d\mathbf{r} \int \int_{E \geq E'} dE dE' [H_{\alpha}(\mathbf{r}, E) - H_{\alpha}(\mathbf{r}, E')]^2 \langle S^T(\mathbf{r}; E, E') \rangle. \quad (17)$$

C. Transfer function

The transfer function $H_\alpha(\mathbf{r}, E)$ is defined as a small-signal response in the electron flux out of contact α to a unit electron in-scattering rate at (\mathbf{r}, E) . Since zero-frequency fluctuations are considered here, any consideration of transient effects is not necessary. Once a small amount of electron in-scattering rate is additionally introduced in the device under steady state, the device will reach another steady state slightly different from the original one. Then the difference of physical quantities between the two steady states is used to calculate the transfer function. To calculate this small-signal problem efficiently, we employ the Langevin approach which provides a set of linearized transport equations from the original ones.²⁻⁴ Here we can neglect the fluctuation of the retarded Green's function and exclude the hole part of the equations. Then we obtain NEGF-Langevin equations from the steady-state NEGF equations,¹⁶

$$\delta\Gamma^{in}(\mathbf{r}, E; \mathbf{r}_0, E_0) = \int d\mathcal{E} D(\mathcal{E}) \delta n(\mathbf{r}, E + \mathcal{E}; \mathbf{r}_0, E_0) + \frac{\hbar}{p(\mathbf{r}_0, E_0)} \delta(\mathbf{r} - \mathbf{r}_0) \delta(E - E_0), \quad (18)$$

$$\delta n(\mathbf{r}, E; \mathbf{r}_0, E_0) = \frac{1}{2\pi} \int d\mathbf{r}' |G^r(\mathbf{r}, \mathbf{r}'; E)|^2 \delta\Gamma^{in}(\mathbf{r}', E; \mathbf{r}_0, E_0), \quad (19)$$

where the second term in Eq. (18) is the Langevin source responsible for a unit electron in-scattering rate at (\mathbf{r}_0, E_0) . After solving the above two equations in the entire space and energy domains, we obtain the transfer function for the contact α as

$$H_\alpha(\mathbf{r}_0, E_0) = \frac{1}{2\pi\hbar} \int dE \int \int_{\mathbf{r} \in \Omega_\alpha} d\mathbf{r} d\mathbf{r}' |G^r(\mathbf{r}, \mathbf{r}'; E)|^2 \Gamma^{out}(\mathbf{r}, E) \delta\Gamma^{in}(\mathbf{r}', E; \mathbf{r}_0, E_0). \quad (20)$$

Note that the above equations are not responsible for the electron injection on the contacts. It should be assumed that any impulse in one contact cannot propagate to the other, so $H_\alpha(\mathbf{r}, E)$ is set to be unity at the contact α and be zero at the other contacts.

III. SIMULATION RESULTS AND DISCUSSIONS

The structure of the simulated SNWTs is shown in Fig. 1. The diameter of the silicon body (D_{si}) is 4 nm and the gate oxide thickness (T_{ox}) is 1 nm. The lengths of the source (L_S), drain (L_D), and channel (L_G) regions are 10 nm each. The source and drain regions are n -type doped to $10^{20}/\text{cm}^3$ and the channel region is assumed to be intrinsic. The gate work function is set to 4.29 eV to achieve an adequate threshold voltage. The silicon nanowire is along the [100] orientation, the lattice temperature (T) is fixed at 300 K, and $V_S=0$ V. In the simulation the effective-mass approximation is assumed

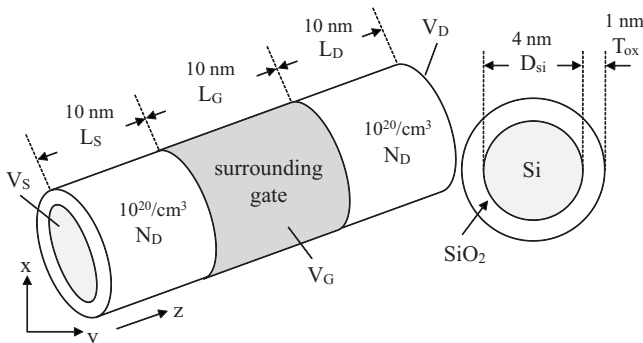


FIG. 1. Structure of the simulated silicon nanowire transistor.

for the six valleys of silicon conduction band with $m_t = 0.19m_0$ and $m_l = 0.98m_0$, where m_0 is the electron rest mass. We further assume that there is no gate current through oxide tunneling, which enables us to treat the transport along the z direction and the quantum confinement in the x - y plane separately from the z direction. Each quantized energy mode due to the transverse quantum confinement effect provides a channel for electron propagation, and we employ the mode-space approach¹⁷⁻¹⁹ to calculate the Green's functions efficiently. For the Poisson equation the gate contact is set by Dirichlet boundary condition, whereas the others are set by Neumann boundary condition. The I_D versus V_G and the I_D versus V_D characteristics are plotted in Fig. 2, which are similar to the conventional MOSFETs with threshold voltage about 0.3 V.

First of all we check whether Eq. (17) satisfies the Johnson-Nyquist theorem that the current noise power at equilibrium should be $4k_B T G_{eq}$ with G_{eq} being the equilibrium conductance.^{23,24} This is a convenient way of setting up noise simulations without comparing with experimental data. In Fig. 3, we confirm that the drain current noise power converges to the equilibrium noise level as the considered number of ensembles increases. The convergence criteria depend mostly on the injection noise contribution, and in this case several hundreds of ensembles are needed to obtain well-converged data. The convergence speed and the proportion of noise contributions can be different from devices and situations.

Unlike the equilibrium noise, the nonequilibrium noise is not determined by the conductance measurement only but related to the details of electronic transport in the device. Among various noise features we are especially interested in the shot noise whose power is proportional to

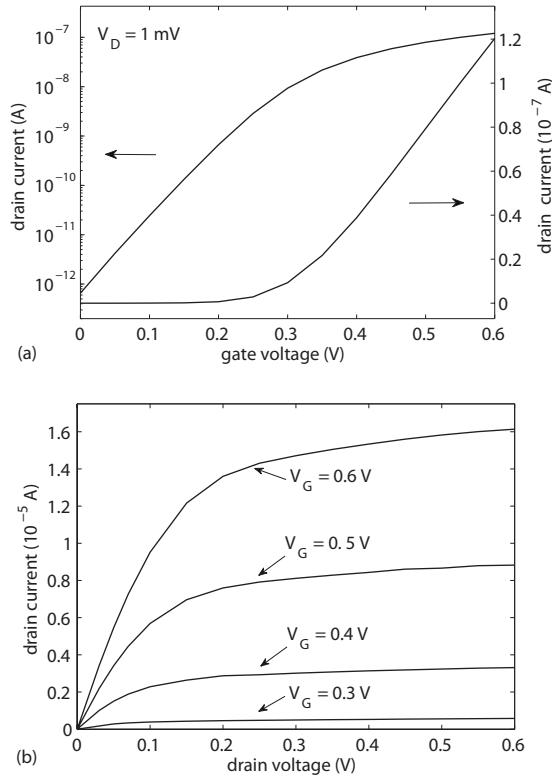


FIG. 2. (a) I_D vs V_G in the linear and log scales and (b) I_D vs V_D characteristics of the simulated silicon nanowire transistor. The threshold voltage is around $V_G=0.3$ V.

the current. Shot noise is manifested when the electrons contributing to the current flow unilaterally, randomly, and independently.^{16,25} Roughly speaking, the condition of unilaterality depends on the magnitude of applied bias, the condition of randomness is guaranteed by electron-phonon interactions, and the condition of independence depends on the strength of electron-electron correlations like the Pauli exclusion principle and the long-range Coulomb interactions. If these conditions are satisfied, the fluctuation of the current follows the Poisson process and its maximum power is equal to the current with a factor of $2e$ in a stable system due to the particle nature of electrons.²⁶

In Fig. 4 we plot the drain current noise and its contributing components with respect to the drain voltage in the weak-inversion regime, where the full shot-noise level and the drain current noise without the long-range Coulomb interactions are also plotted. As the drain bias is increased above the thermal voltage, a unilateral transport of electrons from the source to the drain is induced and then the drain current noise becomes like shot noise. If there were no electron-electron correlations in the device, full shot noise would be observed in the drain current with a large applied drain voltage. However the electron-electron correlations in the channel region are not negligible even in the weak-inversion regime, which suppress the shot noise by about 10%. By comparing the full shot-noise level and the drain current noise with and without the long-range Coulomb interactions, we can estimate the shot-noise suppressions due to the Pauli exclusion principle and the long-range Coulomb interactions are 1% and 9%, respectively.

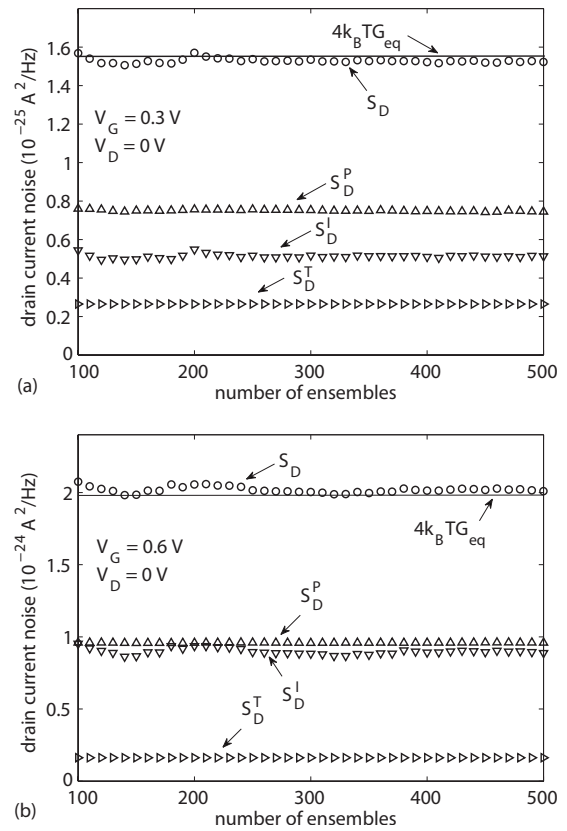


FIG. 3. Drain current noise and its contributing components with respect to the number of ensembles at equilibrium with (a) $V_G=0.3$ V and (b) $V_G=0.6$ V. Theoretically estimated equilibrium noise ($4k_B T G_{eq}$) is obtained by extracting equilibrium conductance from dc simulations.

Figure 5 plots the drain current noise and its contributing components with respect to the drain voltage in the strong-inversion regime. Unlike the weak-inversion regime, the significant shot-noise suppression by about 33% is observed even when the large drain bias is applied, which is due to the increased electron-electron correlations in the channel re-

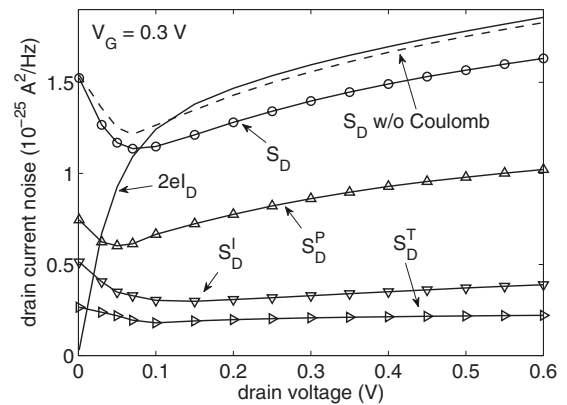


FIG. 4. Drain current noise and its contributing components with respect to the drain bias in the weak-inversion regime ($V_G=0.3$ V). The shot-noise suppression due to the Pauli exclusion principle and the long-range Coulomb interactions are 1% and 9%, respectively.

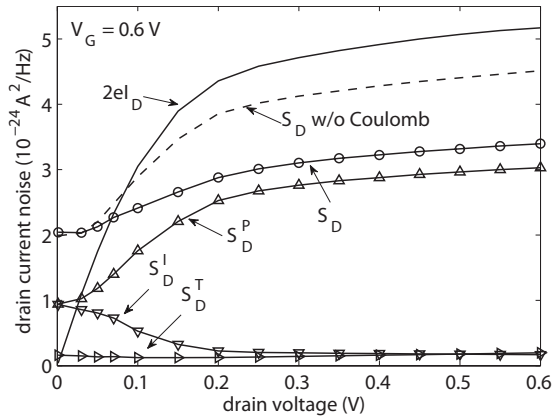


FIG. 5. Drain current noise and its contributing components with respect to the drain bias in the strong-inversion regime ($V_G = 0.6$ V). The shot-noise suppression due to the Pauli exclusion principle and the long-range Coulomb interactions are 12% and 21%, respectively.

gion. Similar to our results, a significant shot-noise component in the drain current has been also reported in the short-channel MOSFETs experimentally.²⁷ For the long-channel MOSFETs, however, the drain current noise power in the saturation regime is known to remain at approximately two third of the equilibrium noise power.^{1,3,28}

When interested in the suppression of shot noise, it is convenient to define the Fano factor as the ratio of the drain current noise to the full shot-noise level ($S_D/2eI_D$). Figure 6 plots the Fano factor and its contributing components with respect to the gate voltage, where we can see different aspects of the drain current noise below and above the threshold voltage. The suppression of the shot noise above the threshold voltage is due to the increase in the electron-electron correlations in the channel region as the electron density is increased in the region. We notice that the Fano factor of the drain current noise of SNWTs in the presence of electron-phonon interactions is predicted to be larger than that of the ballistic transport limit shown in Refs. 15 and 25, which seems to be due to the broadening effect that reduces the Pauli exclusion principle. However the drain current noise seems to be loosely dependent on the electron-phonon interactions. This is true as long as electron-phonon interactions do not change the transport characteristics significantly since electron-phonon interactions just interfere and relay the flow of electrons injected from the other electrons-phonon interactions. Electron-phonon scattering can be a dominant transport mechanism in some devices and then we expect it to have a strong influence on noise.

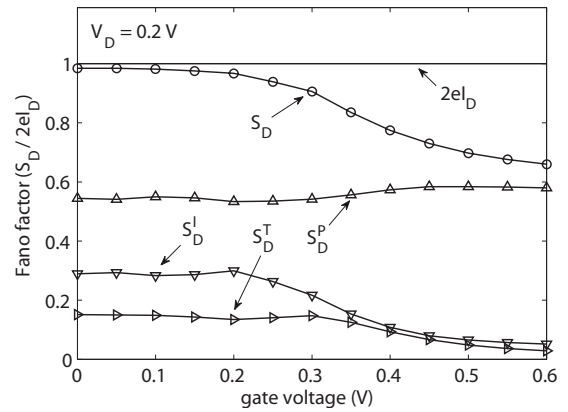


FIG. 6. Gate bias dependence of the Fano factor ($S_D/2eI_D$) and its contributing components with a large drain voltage ($V_D = 0.2$ V). Shot-noise suppression depends on the strength of electron-electron correlations which changes drastically around the threshold voltage ($V_G = 0.3$ V).

IV. CONCLUSION

We have presented a general quantum approach to electronic noise calculations for nanoscale devices. The suggested method is based on the nonequilibrium Green's-function formalism with electron-phonon interactions and takes the effects of the Pauli exclusion principle and the long-range Coulomb interactions into account. As examples we analyzed the drain current noise characteristics of silicon nanowire transistors at room temperature, where the full shot noise is observed in the subthreshold regime with the large drain voltage and is suppressed significantly in the strong-inversion regime due to the Pauli exclusion principle and the long-range Coulomb interactions. We also have discussed the condition of manifestation of shot noise and the role of electron-phonon interactions on noise.

ACKNOWLEDGMENTS

This work was partially supported by NSF under Grant No. EEC-0228390 that funds the Network for Computational Nanotechnology, by NSF PetaApps under Grant No. 0749140, by the Nanoelectronics Research Initiative (NRI) through the Midwest Institute for Nanoelectronics Discovery, by the Materials Structures and Devices Focus Center (MSD) funded by Focus Center Research Program (FCRP), by the National Research Foundation of Korea Grant funded by the Korean Government (Grant No. NRF-2009-352-D00114), and by Purdue University nanoHUB.org computational resources such as the “workspace application” have been used in this work.

¹A. van der Ziel, *Noise in Solid State Devices and Circuits* (Wiley, New York, 1986).

²S. Kogan, *Electronic Noise and Fluctuations in Solids* (Cambridge University Press, New York, 1996).

³F. Bonani and G. Ghione, *Noise in Semiconductor Devices, Modeling and Simulation* (Springer-Verlag, Berlin, 2001).

⁴C. Jungemann, *IEEE Trans. Electron Devices* **54**, 1185 (2007).

⁵G. B. Lesovik, *JETP Lett.* **49**, 594 (1989).

⁶B. Yurke and G. P. Kochanski, *Phys. Rev. B* **41**, 8184 (1990).

⁷M. Büttiker, *Phys. Rev. Lett.* **65**, 2901 (1990).

⁸L. Y. Chen and C. S. Ting, *Phys. Rev. B* **43**, 4534 (1991).

⁹R. Landauer and Th. Martin, *Physica B* **175**, 167 (1991).

- ¹⁰M. Büttiker, *Phys. Rev. B* **46**, 12485 (1992).
- ¹¹G. Iannaccone, M. Macucci, and B. Pellegrini, *Phys. Rev. B* **55**, 4539 (1997).
- ¹²J.-X. Zhu and A. V. Balatsky, *Phys. Rev. B* **67**, 165326 (2003).
- ¹³M. Galperin, A. Nitzan, and M. A. Ratner, *Phys. Rev. B* **74**, 075326 (2006).
- ¹⁴V. N. Do, P. Dollfus, and V. L. Nguyen, *Appl. Phys. Lett.* **91**, 022104 (2007).
- ¹⁵A. Betti, G. Fiori, and G. Iannaccone, *Phys. Rev. B* **81**, 035329 (2010).
- ¹⁶H.-H. Park, S. Jin, H. S. Min, and Y. J. Park, *J. Appl. Phys.* **105**, 023712 (2009).
- ¹⁷E. Polizzi and N. Ben Abdallah, *Phys. Rev. B* **66**, 245301 (2002).
- ¹⁸J. Wang, E. Polizzi, and M. Lundstrom, *J. Appl. Phys.* **96**, 2192 (2004).
- ¹⁹S. Jin, Y. J. Park, and H. S. Min, *J. Appl. Phys.* **99**, 123719 (2006).
- ²⁰S. Datta, *J. Phys.: Condens. Matter* **2**, 8023 (1990).
- ²¹M. J. M. de Jong and C. W. J. Beenakker, *Mesoscopic Electron Transport*, NATO Advanced Studies Institute Series E Vol. 345 (Kluwer Academic, Dordrecht, 1997), p. 225.
- ²²T. González, O. M. Bulashenko, J. Mateos, D. Pardo, and L. Reggiani, *Phys. Rev. B* **56**, 6424 (1997).
- ²³J. B. Johnson, *Phys. Rev.* **32**, 97 (1928).
- ²⁴H. Nyquist, *Phys. Rev.* **32**, 110 (1928).
- ²⁵H.-H. Park, S. Jin, Y. J. Park, and H. S. Min, *J. Appl. Phys.* **104**, 023708 (2008).
- ²⁶Ya. M. Blanter and M. Büttiker, *Phys. Rep.* **336**, 1 (2000).
- ²⁷M. S. Obrecht, E. Abou-Allam, and T. Manku, *IEEE Trans. Electron Devices* **49**, 524 (2002).
- ²⁸H. C. de Graaf and F. M. Klaassen, *Compact Transistor Modeling for Circuit Design* (Springer-Verlag, Wien, 1990).